Science of the Total Environment 612 (2018) 694–707

Contents lists available at ScienceDirect

Science of the Total Environment

journal homepage: www.elsevier.com/locate/scitotenv

A mobile pool of contaminated sediment in the Penobscot Estuary, Maine, USA

W. Rockwell Geyer *, D.K. Ralston

Woods Hole Oceanographic Institution, United States

HIGHLIGHTS

- The Penobscot estuary exhibits a "mobile pool" of mobile sediments that causes the homogenization of contaminants.
- The mobile results in a long residence time and thus a long recovery timescale for contaminants.
- The principal cause of the mobile pool is a episodic remobilization of sediment due to seasonal variations in river discharge.

GRAPHICAL ABSTRACT

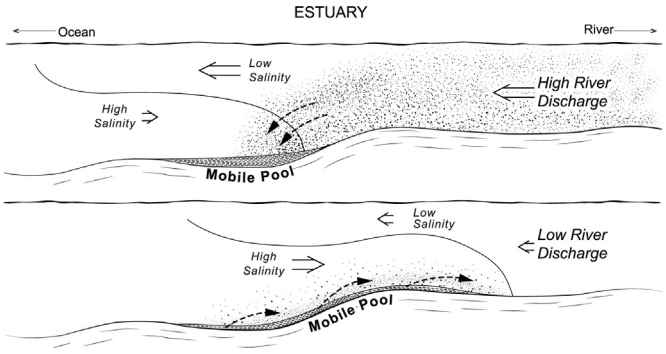

ARTICLE INFO

Article history:
Received 3 May 2017
Received in revised form 21 July 2017
Accepted 22 July 2017
Available online xxxx

Editor: D. Barcelo

Keywords:
Contaminated sediment
Estuary
Residence time
Mobile pool
Resuspension

ABSTRACT

The natural recovery of estuaries from contamination is largely determined by the timescale over which contaminated sediment is exported or buried and replaced by cleaner sediment that enters from the watershed or the ocean. That timescale depends on the size of the "pool" of contaminated sediment that resides in the estuary. The larger the pool, the longer the recovery timescale for a given rate of sediment input. A field study was undertaken as part of a study of mercury contamination in the Penobscot estuary to assess the mechanisms affecting the transport and fate of contaminated sediment. Based on measurements of water properties, currents and sediment transport and seabed samples analyzed for sediment properties and contaminant concentrations, a "mobile pool" of contaminated sediment with relatively uniform geochemical characteristics along a 20-km reach of the estuary was identified. This pool of sediment is mobilized seasonally by resuspension and trapping processes associated with salinity fronts that vary in location with discharge conditions. Sediment is transported down-estuary during high discharge and up-estuary during low discharge, with seasonal, bi-directional transport of sediment in the estuary significantly exceeding the annual input of new sediment from the watershed. This continual, bi-directional transport leads to homogenization of the chemical properties of the mobile sediment, including contaminant concentrations. The large mass of mobile sediment relative to the input of sediment from the watershed helps explain the long recovery timescale of contaminants in the Penobscot estuary.

1. Introduction

Estuaries tend to trap sediment, due to the convergence of flow associated with the estuarine circulation (Postma, 1967; Schubel, 1968). Although sediment transport and trapping occurs in the water column,

* Corresponding author.
E-mail address: rgeyer@whoi.edu (W. Rockwell Geyer).

http://dx.doi.org/10.1016/j.scitotenv.2017.07.195
0048-9697/

most of the sediment usually resides on the seabed and is periodically resuspended by tidal motions (Wellershaus, 1981; Grabemann et al., 1997). Schoellhamer (2011) identifies this mass of erodible sediment based on long-term observations of sediment transport in San Francisco Bay, finding that the size of that pool may be much larger than the amount of sediment that is resuspended at any given time. Observations in other estuaries support the concept of an erodible pool, or what this paper will refer to as a "mobile pool" of sediment. Migniot (1971) observed seasonal changes in bed elevation in the Gironde estuary of as much as 2 m due to sediment trapping and remobilization in association with the variation of the position of the salt intrusion. Woodruff et al. (2001) found a similar regime in the Hudson estuary, in which a mass of sediment comparable to the annual input from the watershed was redistributed between depositional zones separated by 10–15 km along the lower estuary. During high flow conditions, sediment accumulated in the seaward reaches, and during lower discharge periods it would be remobilized and deposited in more landward depositional areas. Observations in the tidal salt wedge of the Connecticut River also found seasonal shifts in the distribution of deposition of fine sediment from the lower estuary during high discharge to more landward side embayments during lower discharge conditions, a period when sediment input from the watershed was minimal (Yellen et al., 2017; Valentine et al., submitted).

The mobile pool should not be confused with the "fluff layer" (Maa et al., 1998), a thin layer (on the order of millimeters) of loosely aggregated sediment that is readily remobilized by tidal resuspension. The mobile sediment pool is potentially much thicker, as a result of cycles of net erosion and deposition that persist over much longer timescales than the tides. For example, Migniot's (1971) observations in the Gironde indicated mobile sediment thickness on the order of 1 m, and a similar thickness of mixed sediment was observed by Kuehl et al. (1986) in the estuarine regime at the mouth of the Amazon River. In order for such a thick layer of sediment to be remobilized, not only must repeated episodes of sediment resuspension occur, but the pool of mobile sediment must be relocated from one horizontal position in the estuary to another. Even energetic estuaries only remobilize millimeters to at most several cm of bed sediment in individual tidal cycles (e.g., Traykovski et al., 2004). Moreover, this relocation must be bi-directional and quasi-cyclical over some timescale significantly longer than the tides to result in the homogenization of a pool of sediment. The quasi-cyclical variation of sediment transport is most often the result of seasonal or episodic variations in river flow (Migniot, 1971; Woodruff et al., 2001), but it may also may result from seasonal changes in wind or wave forcing (Kuehl et al., 1986).

The mobile sediment pool has important consequences for the long-term fate of contaminants in estuaries. Persistent contaminants such as mercury and polychlorinated bi-phenols (PCBs) tend to be highly particle-reactive and associated with fine particles (Feng et al., 1998; Israelsson et al., 2014). We hypothesize that the presence of a mobile sediment pool may significantly increase the timescale for natural recovery of a contaminated estuary, due to the trapping of contaminants within a large reservoir of sediment. Multiple cycles of resuspension, transport and deposition also homogenize the chemical properties of the sediment within the pool, leading to relatively uniform contaminant concentrations and potentially erasing the spatial and temporal information on the sources of contamination to the estuary.

The Penobscot estuary provides an example of an estuary where contaminants that were released decades ago continue to affect environmental quality. The Penobscot experienced significant loading of mercury from an industrial facility in the upper estuary between the 1960s and 1970s (Bodaly et al., this volume; Turner et al., this volume), which has resulted in contamination of the sediments within the estuary and adjacent marshes, most notably Mendall Marsh (Fig. 1). The dominant form of mercury in the Penobscot is inorganic mercury (Bodaly et al., this volume), as in other contaminated estuarine environments (Mason et al., 1999; Cardona-Marek et al., 2007). Once in the estuarine environment, the transport and fate of mercury is closely tied to the transport of sediment, due to the strong affinity of mercury to particles (Cardona-Marek et al., 2007). Therefore the fate of mercury is closely tied to the fate of particles within estuaries, with burial and export of contaminated sediment representing the main sinks that balance the inputs of mercury from the watershed, industrial sites and the atmosphere (Mason et al., 1999). The mercury contamination of the Penobscot is dominated by a single industrial source with a well quantified and relatively compressed temporal signal, so the observations of mercury in the Penobscot estuary provide an effective case study illustrating the influence of a mobile sediment pool on the distribution of contaminants in an estuary.

As part of the Penobscot River Mercury Study, a field investigation was conducted of the physical transport processes that affect the transport and fate of contaminated sediment in the estuary. This paper reports on the results of that transport study, and on evidence of a mobile sediment pool within the Penobscot estuary based on moored and shipboard measurements of physical transport processes as well as sedimentological and chemical analysis of sediment bed samples.

2. Observational program

2.1. Site description

The Penobscot River is the largest river in the state of Maine, with a watershed size of 22,000 km and an annual average discharge of approximately 350 $m^3\ s^{-1}$. Peak annual discharge averages 1800 $m^3\ s^{-1}$, and the low-flow minimum is around 150 $m^3\ s^{-1}$. Salinity within the estuary ranges from 0 to 30 psu, and temperatures range from 0–20 °C through the annual cycle. The estuary extends 35 km seaward from the limit of tidal influence at Veazie Dam near Bangor southward to Fort Point, where the estuary opens up into Penobscot Bay (Fig. 1), which joins the Gulf of Maine 50 km to the south of the estuary. For the purpose of this paper Fort Point will be considered the mouth of the estuary, with distances referenced from there. The estuary has a complex morphology due to the influence of glacial processes on the highly resistant bedrock. The estuary has highly variable depth, from several meters in the shoals to more than 30 m in incised channels between bedrock outcrops. The channel depth decreases near Bucksport (km 13) from 20 m to about 10 m, and the channel depth of around 10 m continues up to km 35. Several shallow embayments join the estuary at small lateral tributaries, including Mendall Marsh and the Orland River, and the estuary bifurcates around Verona Island, with the deeper main channel passing to the west of the island.

The tidal range, is as much as 4.9 m during spring tides and 2.9 m during neap tides. Tidal velocities are close to 1 m/s through much of the domain, with a typical neap-to-spring range of 0.7 to 1.3 m/s. The freshwater inflow leads to strong salinity stratification and strong horizontal salinity gradients, with variability at the seasonal and event time scales of river discharge. During low flow conditions, salt extends all the way to km 35 near Bangor, and during moderate to high flow conditions, the upper estuary above km 20 is fresh. Smaller tributaries entering through side embayments provide minimal freshwater inflow, only influencing the conditions within the embayments themselves.

2.2. Description of observations

Measurements of the hydrodynamics, water properties and sediment transport in the estuary were obtained during field efforts in the spring of 2010 and in the spring and summer of 2011. Time series measurements included bottom tripods with upward-looking acoustic Doppler current profilers (ADCPs) manufactured by Teledyne, Inc., conductivity-temperature-depth (CTD) sensors and optical backscatter sensors (OBSs) manufactured by RBR Limited. The tripods were placed at 6 locations in the estuary in 2010 and 2 locations in 2011 (Fig. 1). CTDs and OBSs measured water properties 0.6 m above the bottom.

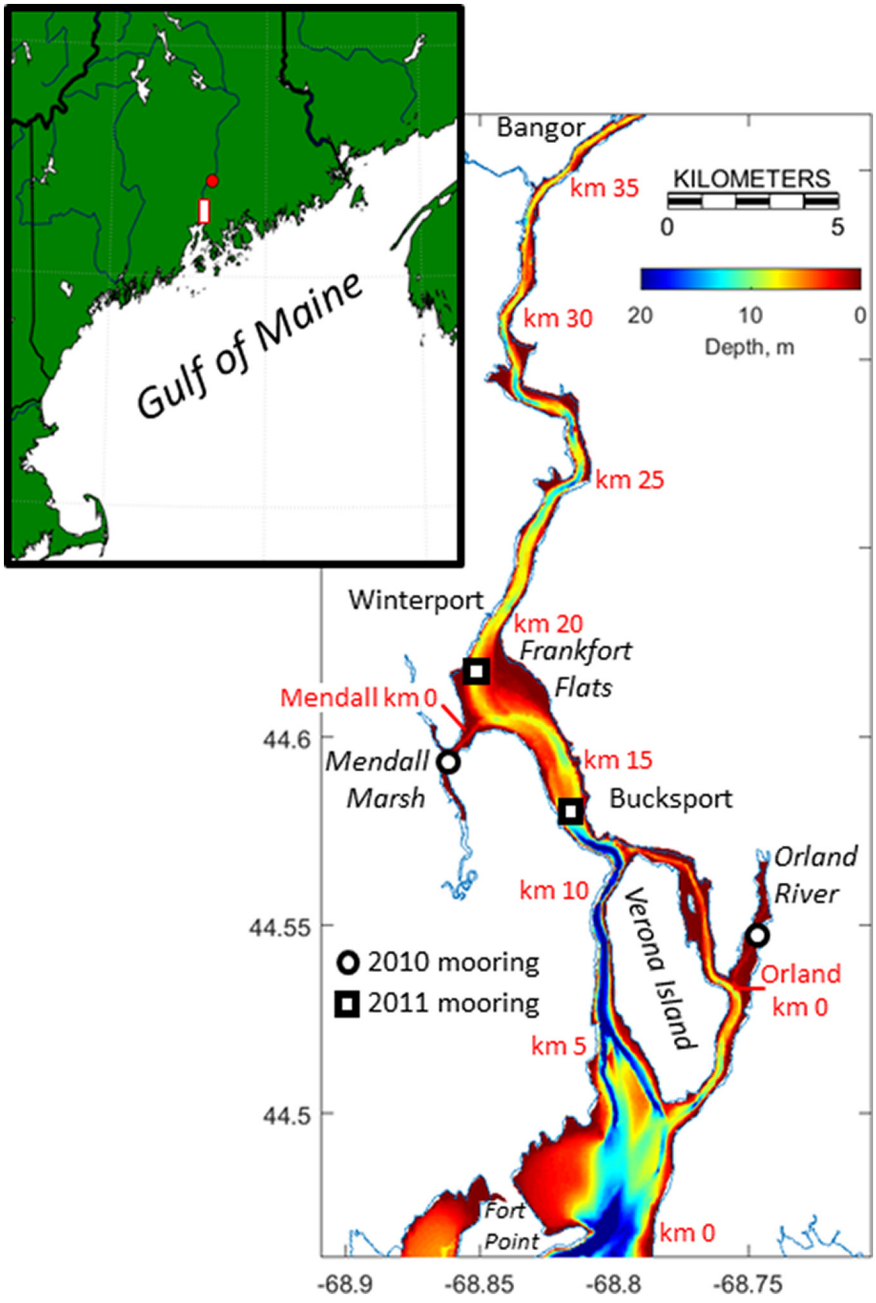

Fig. 1. The Penobscot River estuary, showing locations of the moorings in 2010 and 2011. The inset shows the location of the study area relative to the Gulf of Maine. Bathymetry is indicated by the color scale. Distances along river in km are indicated. The origins (km 0) of the Mendall and Orland transects are also indicated. The red dot on the inset map shows the location of Veasie Dam. (For interpretation of the references to color in this figure legend, the reader is referred to the web version of this article.)

The bottom-most velocity measurements were approximately 1 m above bottom, and velocity profiles above that were measured at 0.2–0.5 m increments, depending on the station depth. Acoustic backscatter was also recorded through the water column and converted to suspended sediment concentration based on a calibration with shipboard sediment concentration measurements (see below). Surface moorings had temperature-salinity and optical backscatter sensors mounted 0.5-m below the water surface. Optical backscatter was converted to suspended sediment concentration based on water samples that were analyzed in the lab for total suspended solids.

During the 2011 observations, the velocity and water property measurements indicated that the bottom tripod at the Bucksport location was abruptly buried by sediment several days after the deployment. This tripod was located in the most intense sediment trapping zone in the estuary, as subsequently revealed by shipboard surveys. The tripod remained completely buried as of the scheduled recovery in June 2011, and after several unsuccessful recovery attempts through the summer of 2011, the sediment eventually shifted enough to partially uncover the tripod so it could be recovered with the assistance of divers in August 2011. The interpretation and implications of the burial are discussed in Section 4.

Shipboard surveys used a combination of ADCP measurements (for currents and acoustic backscatter) and profiling with a CTD and OBS. A 1.2 l Nisken bottle with a bottom-actuated trigger was used to obtain water samples for calibration of the suspended sediment. A total of 263 bottom water samples and 107 surface samples were filtered with 0.45 μm fiberglass filters and weighed to determine suspended sediment concentrations. The range of suspended sediment concentrations

based on the bottle samples was from less than 1 to more than 2000 mg/l for the near-bottom samples, and 0–200 mg/l for the surface samples.

The relationship between concentration and optical backscatter for the near-bottom samples was found to be nonlinear, so a 3rd order polynomial was fit to the data, yielding a regression coefficient $r^2 = 0.85$. For concentrations less than 200 mg/l, the regression was approximately linear, with a relationship C (mg/l) = FNU × 2.14 (where C is suspended sediment concentration and FNU is Formazin Nephelometric Units measuring turbidity.) The surface samples had a linear relationship with C (mg/l) = FNU × 1.65 (with $r^2 = 0.95$ after discarding 7 points that had anomalously high backscatter, probably due to near-surface bubbles). The difference in the regression between near-surface and near-bottom samples may be associated with differences in grain-size distribution of the near-surface and near-bottom sediment, and is consistent with larger particles that scatter light less effectively relative to their mass in the near-bottom samples (Downing, 2006). Likewise the nonlinear response for high concentrations is likely due to increased coarse material in suspension during times of peak currents, thus altering the calibration during the times of peak observed backscatter. Note that the nonlinear calibration slightly reduces the estimates of concentration and sediment load from a linear calibration.

A limited set of bed sediment samples were obtained in 2010 and more extensive sampling was performed in August 2011. Bed sediment samples were collected during shipboard surveys using a Petit Ponar grab sampler. The depth of penetration of the grab sampler was 6–10 cm into the sediment. For samples with a significant mud fraction to provide cohesion, the surface of the bed sediment was usually identifiable. A sub-sample representing the top 3 cm when identifiable, or a representative subsample of all the bed material otherwise, was saved for grain size analysis. Grain size analysis was performed by wet and dry sieving (Folk and Ward, 1957). The organic fraction of the sediment samples was determined by loss on ignition, determined by heating sub-samples in an oven at 550 °C for 4 h. During the 2011 sampling, part of the subsample was processed for mercury concentration. Total mercury in sediments was determined by EPA method 7473, using a Direct Mercury Analyzer (DMA-80) at Flett Research Ltd., in Winnipeg, Canada. Nominal detection limit was 1.3 ng/g and with a minimum detectable limit of 0.4 ng/g. Recovery of spiked samples (12 determinations) ranged from 97.2–103.8%, median 99.6%, mean 100.4%. Determination of standards (MESS-2; Marine sediments, Beaufort Sea, National Research Council, Canada) (12 determinations) averaged 100.2% (range 97.2–103.3%; median 100.1%).

River discharge measurements were obtained from the USGS gauge at West Enfield, Maine, upstream of the zone of tidal influence. Optical measurements of turbidity obtained by the USGS at Eddington, just above the tidal limit, were calibrated with 18 water samples. The regression produced a relationship C (mg/l) = FNU × 1.77, similar to the near-surface calibration in the estuary, with a regression coefficient of $r^2 = 0.99$. A sediment discharge curve was constructed by obtaining a fit between concentration at Eddington and river discharge for observations between March 2010 and February 2011 (Fig. 2). Although the data set was very short and included only a handful of high discharge data, it is the only set of calibrated field data available to constrain the loading estimate of the river. Following Nash (1994), a power law fit was sought to maximize the regression between discharge and concentration, based on the expression $C = aQ^b$ where C is the concentration in the river and Q is the river discharge. The best fit was found for an exponent $b = 1.8$ and $a = 7.7 \times 10^{-3}$, with regression coefficient $r^2 = 0.74$. Woodruff et al. (2013) found a similar exponent of 1.9 for the nearby Connecticut River, although the average concentrations of the Connecticut tend to be higher.

The regression curve provides only a crude estimate of the sediment loading; indeed the concentration-discharge relationship is expected to vary through individual events and between events (Williams, 1989).

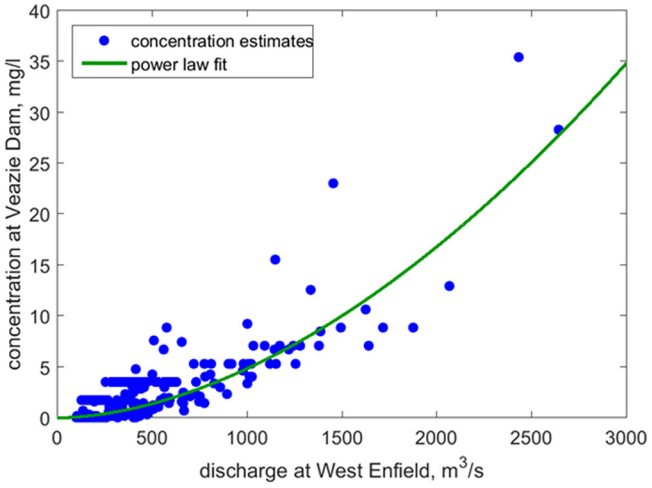

Fig. 2. Relationship between concentration and river discharge for the Penobscot river, showing a power-law fit to the data: $C = aQ^b$ where $a = 7.7 \times 10^{-3}$ and the exponent $b = 1.8$.

3. Results and analysis

3.1. Fluvial processes

River discharge during 2010 and 2011 (Fig. 3) exhibited peak freshets of 1500 to 2000 $m^3\ s^{-1}$. The 2011 period was wetter overall, with multiple discharge peaks extending though year day 150 (end of May). The cumulative sediment load (Fig. 4) was calculated based on the discharge rating curve. As noted above the regression curve provides only a rough estimate of riverine loading, as it is not based on direct measurement of sediment discharge. Keeping in mind the limitations of the regression estimates, the sediment loading during the 2010 and 2011 freshets was in the range of 20,000–40,000 tons, with likely greater loading during the more intense the 2011 freshet.

3.2. Estuarine salinity distribution and suspended sediment

The observations on April 15 (Fig. 5 upper panels) illustrate high flow conditions ($Q = 1500\ m^3\ s^{-1}$) and intermediate tidal range (3.8 m), during which the Penobscot estuary has the structure of a tidally forced salt wedge (Geyer and Farmer, 1989; Ralston et al., 2010), with strong stratification and a distinct bottom salinity front during the flood tide that extends to the vicinity of Mendall Marsh (km 20). During the ebb (Fig. 5, 2nd panel), the salt wedge collapses due to

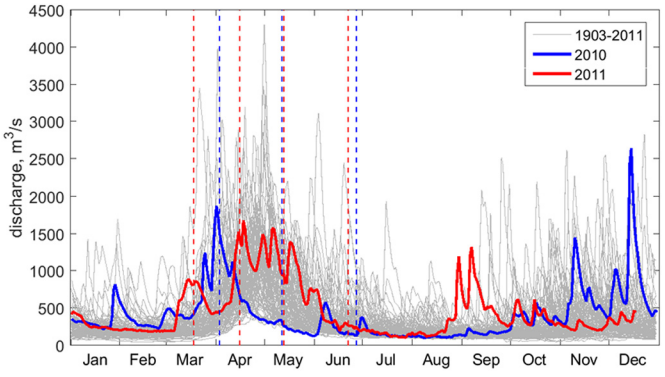

Fig. 3. Discharge of the Penobscot at Enfield, ME, during 2010 and 2011, overlain on discharge curves between 1903 and 2011. The times of the shipboard surveys in 2010 and 2011 are shown by color-coded dashed vertical lines. (For interpretation of the references to color in this figure legend, the reader is referred to the web version of this article.)

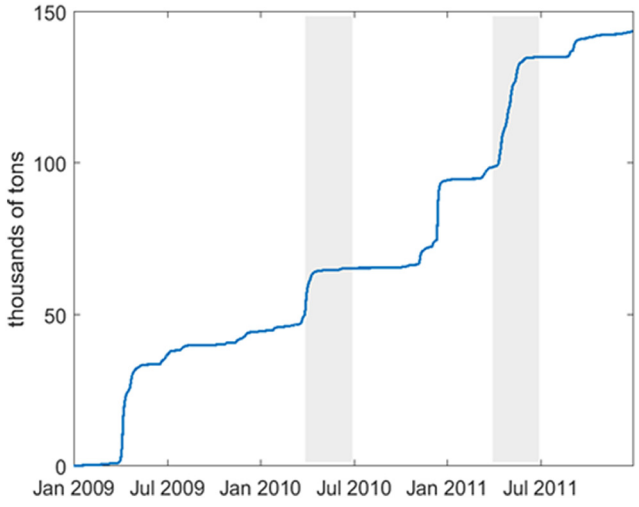

Fig. 4. Integrated sediment loading from the river, based on the power-law regression relationship shown in Fig. 2. The observation periods of 2010 and 2011 are shaded.

tidal mixing, and a front forms near Bucksport (km 12), where the channel deepens to more than 20 m. The along-estuary distribution of suspended sediment has two local estuarine turbidity maxima (or ETMs), which are most evident during the late ebb (Fig. 5 2nd panel). One ETM is located near the maximum landward extent of the salt intrusion near km 20, and the other at the location of the ebb-tide front near km 12. The tripod that was buried by at least 1 m of sediment was located at km 13 near this lower ETM, providing additional (albeit anecdotal) evidence of the intense trapping and deposition of sediment in that part of the estuary.

During low discharge conditions (Fig. 5, 3rd and 4th panels), the salt intrusion is still strongly stratified, but the horizontal salinity gradients are weaker than during high flow and the salt advances much farther up the estuary This variation in position of the salt intrusion is to be expected in response to the variation of river discharge (Lerczak et al., 2009). Enhanced salinity gradients still occur near km 12 and km 20, corresponding to the ETM locations that were observed during high flow conditions. The suspended sediment concentrations are elevated at these locations, but with considerably lower concentrations than were observed during high flow conditions (note the change in scale of the suspended sediment concentration for the lower panels of Fig. 5). An additional region of enhanced sediment concentration is found farther upriver near the limit of the salinity intrusion at km 30.

3.3. Salinity distribution and suspended sediment in side embayments

Measurements of the salinity structure and suspended sediment were performed in Mendall Marsh and Orland River, motivated by observations of significant contaminant accumulation in these side-embayments (Santschi et al., 2017). The watersheds of these embayments are small, so most of the sediment input would be expected to come from the main stem of the Penobscot. Shipboard surveys during flood tides extending into the Mendall Marsh and Orland River (Fig. 6) indicate salt-wedge-like structure of these sub-estuaries during moderate to high flow conditions, with elevated suspended sediment concentrations in the lower layer. In both cases, relatively high concentrations of suspended sediment are observed near the junction with the Penobscot (km 0 in both cases representing the mouths of the tributaries). The flooding current in the near-bottom waters carries sediment into the sub-estuaries. The mooring data (discussed in the next section) indicate a net flux of suspended sediment into these sub-estuaries from the Penobscot.

3.4. Time series observations of currents and water properties

Moored observations at Frankfort station in the main stem adjacent to Mendall Marsh during the 2011 deployment provide a three-month record of the variability of the currents and water properties that characterize the estuary (Fig. 7). Tidal velocities have near-surface magnitudes as strong as 1.5 m/s and near-bottom magnitudes close to 1 m/s. The residual (non-tidal) velocities show surface outflows ranging from −0.6 to −0.2 m/s, and bottom residual velocities alternate between outflow and inflow of around 0.2 m/s. Comparison with the river discharge data indicates that the periods of bottom outflow occur during peak river discharge (dashed vertical lines), and inflow occurs during intervening periods of low to moderate river flow. The bi-directional flow (in at the bottom, out at the surface) is characteristic of the estuarine circulation (Hansen and Rattray, 1965; MacCready and Geyer, 2010), which is driven by the along-estuary density gradient. The reversal of the estuarine bottom current by strong river outflow events is commonly observed in estuaries subject to variations in river flow (e.g., Lerczak et al., 2009), and it is accompanied by a marked change in the salinity structure, which is discussed next.

The salinity at Frankfort (Fig. 7, middle panel) varies markedly at both at tidal time scales and in association with the river outflow events. The near-bottom salinity varies from 0 to 28 psu, sometimes with as much as 25 psu variation in one tidal cycle, which is indicative of tidal advection of a strong horizontal salinity gradient (cf. Fig. 5). The surface salinity is generally 0 to 10 psu, consistent with the strong, persistent stratification in the shipboard survey data (Fig. 5). Bottom salinity decreases during river outflow events (vertical dashed lines) as the salinity intrusion is pushed seaward by the high river flow and the near-bottom currents reverse. The salinity response lags the velocity by several days due to the finite adjustment timescale of the salinity field.

Suspended sediment at Frankfort (Fig. 7, bottom panel) also varies at both tidal time scales and at lower frequencies. Near-bottom concentrations range from 10 to more than 1000 mg/l on tidal timescales, and the tidally averaged concentrations span 30 to 300 mg/l. The tidal variability corresponds with resuspension of easily eroded sediment that has been trapped in the frontal zone. The low-frequency variability is mainly due to changes in tidal amplitude, with peak concentrations occurring during spring tides that have the maximum near-bottom tidal velocities (Fig. 7, upper panel). River discharge also influences the sediment concentrations, but in a complex way that seems to be related to the variations in sediment trapping in the frontal zone.

Near-surface concentrations are a factor of 4 to 20 lower than near-bottom concentrations, indicative of settling and bottom resuspension. Stratification also suppresses vertical mixing of sediment, keeping near-bottom suspended sediment from reaching the surface (Geyer, 1993). River discharge plays a role in the near-surface sediment concentrations, with the peak near-surface concentrations occurring during or shortly after the peak discharge events.

Looking in more detail at the conditions around peak discharge, we find that the tidally averaged surface concentrations in the estuary (Fig. 7, lower panel) are a factor of 2–4 greater than the estimated concentration in the river for those discharge conditions (Fig. 2). Also note that the maximum ebb concentration during the first discharge peak (around March 20) reach more than 300 mg/l, a factor of 10 greater than the estimated riverine concentration. These high concentrations occur during strong ebbs when the salt front has been displaced seaward of the mooring location and significant resuspension occurs in the upper estuary (Fig. 7, middle panel). The key finding here is that while the fresh water being advected out the estuary during the ebb originated from the river, most of the outgoing suspended sediment originated from resuspension of previously deposited sediment, because its concentration far exceeds what is supplied by the river.

Although the variations in suspended sediment clearly indicate the influence of tidal amplitude and river outflow, the relationship between peak concentrations and the forcing factors varies through the

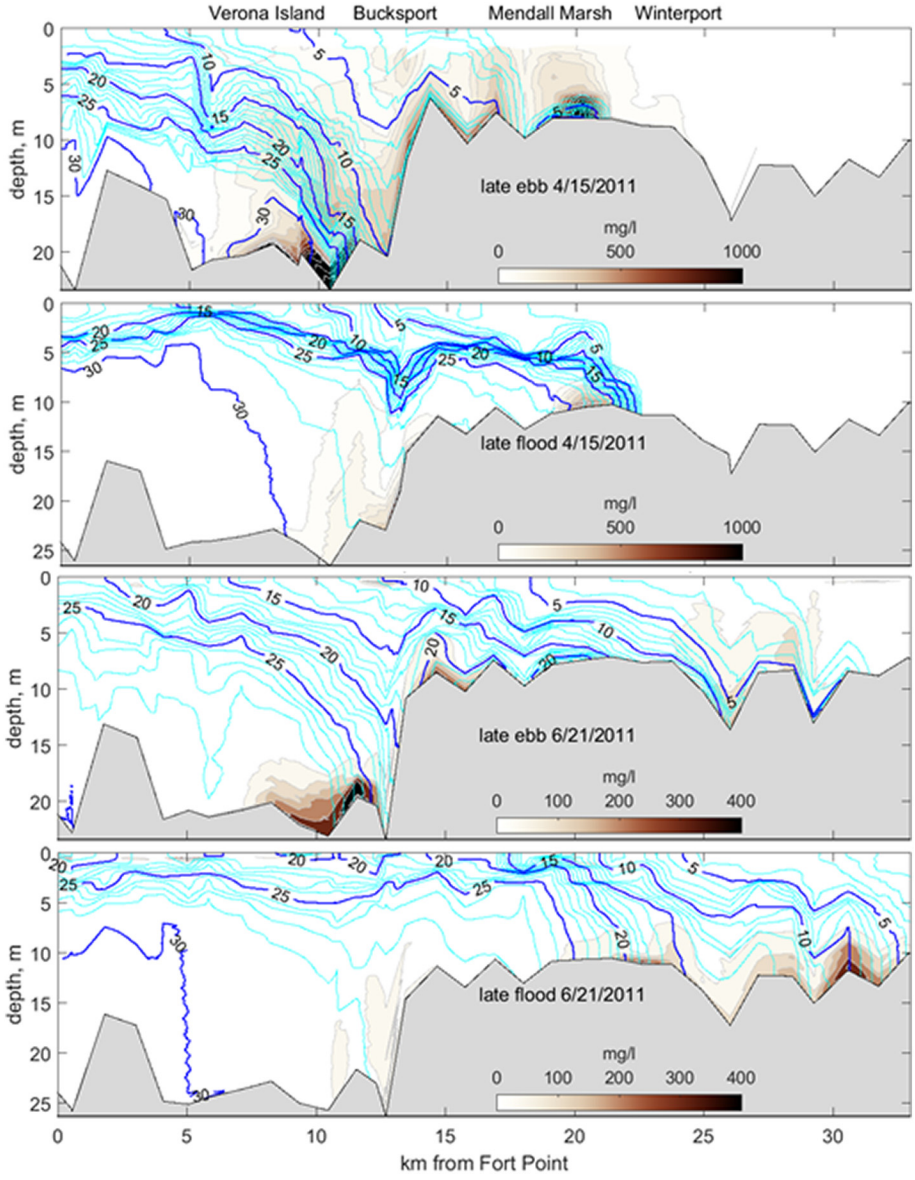

Fig. 5. Cross-sections during high discharge (upper panels) and low discharge (lower panels) along the axis of the Penobscot estuary (the mouth to the left) near the end of late ebb and late flood, showing salinity (psu) in blue contours and suspended sediment (mg/l) with brown shading. The sediment concentration scale changes between the upper and lower panels, reflecting the marked decrease in suspended sediment concentrations during low flow. Note the change in position of the front (zone of closely spaced salinity contours intersecting the bottom) between ebb and flood and between high discharge and low discharge conditions. (For interpretation of the references to color in this figure legend, the reader is referred to the web version of this article.)

observation period. For example, the highest surface suspended sediment concentrations are observed during the first freshet event in March, although the discharge is only half the amplitude of the second event (compare 2011 peaks in Fig. 3) and the tidal conditions are comparable. It is possible that the sediment loading from the river was higher during the first, small freshet peak, due to remobilization of sediment that had been stranded in the river during a the falling limb of the discharge curve (Williams, 1989). However given the large magnitude of this initial sediment flux, a more likely source of this initial pulse of sediment is the sediment that had been trapped in the upper estuary during the previous low-discharge period. This explanation is consistent with the discharge-dependent variation of the estuarine sediment transport regime, which carries sediment to the upper estuary during low flow, whereupon it can be remobilized and carried back down-estuary during high flow. Although the first freshet peak was not particularly strong, it was adequate to shift the estuarine front seaward (as evidenced by the drop in salinity), thus shifting the sediment trapping zone from the upper to the middle estuary. This explanation is consistent with sediment flux estimates and observed bed sediment distributions presented in Sections 3.5 and 3.6. The relationship between the intensity of sediment resuspension and the variation of bottom stress (as parameterized by a quadratic drag law) provides additional evidence for changes in the distribution of erodible sediment during the observation period. If the erodibility of sediment were uniform in time, the concentration would be expected to vary quadratically with near-bed velocity U (e.g., Partheniades, 1965) above some threshold U_c:

$$C_{pred} = C_0 \frac{\left(U^2 - {U_c}^2\right)}{{U_c}^2} \qquad U \geq U_c$$
$$C_{pred} = 0 \qquad U < U_c \tag{1}$$

where C_{pred} is the predicted suspended sediment concentration and C_0 is the reference concentration. Applying this quadratic formula and assuming constant erodibility over the observation period, we find that

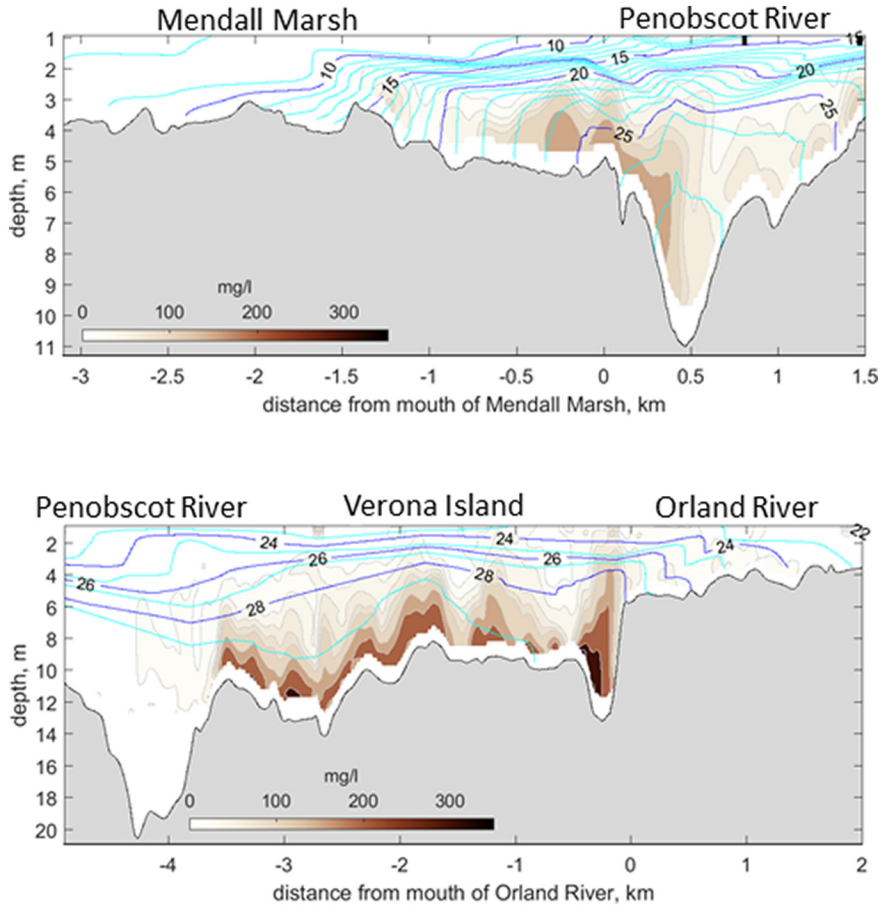

Fig. 6. Cross-sections in the lateral embayments and adjacent portions of Penobscot Bay: Mendall Marsh (upper panel) and the Orland River (lower panel) during May 2010, showing salinity (blue contours) and suspended sediment (brown shading). Note that sediment is trapped in the main stem of the Penobscot in front of each of these embayments. (For interpretation of the references to color in this figure legend, the reader is referred to the web version of this article.)

$C_o = 8$ mg/l and $U_c = 0.13$ m/s provide the best fit to the observed near-bottom concentration, but the quality of fit varies with of time. Sediment concentration is under-predicted at the beginning and end of the record, and over-predicted in the middle. This discrepancy is consistent with the presence of excess erodible sediment (or effectively a greater C_0) at the mooring location at the beginning and end, and a deficit of erodible sediment during the high-discharge period in May. The sediment flux calculations that are discussed in the next section suggest that this variation in sediment availability is explained by a down-estuary shift of the mobile pool during the freshet period, followed by an up-estuary shift during the lower discharge period in late May and June.

3.5. Sediment flux

An estimate of the integrated sediment transport past the mooring was calculated from the time series of velocity and sediment concentration. The measurements were from a single location in the estuarine cross-section and therefore required assumptions about the vertical and lateral structure of the velocity and suspended sediment distributions. Although the assumptions about the lateral structure include uncertainty, the calculation provides a clear indication of the temporal variability of sediment transport and particularly its directionality through the deployment period. For the purpose of the calculation, the lateral distribution of suspended sediment was assumed to be uniform across a width of 300 m (consistent with the channel width), and the vertical distribution of near-bed sediment was assumed to decay exponentially in the vertical (similar to Geyer et al., 2001). Two vertical decay scales were selected, 2-m and 3-m, roughly bracketing the typically observed range of vertical decay scales from the shipboard backscatter profiles. Surface concentrations were matched by imposing an offset to the exponential for each profile, consistent with the presence of a wash load with low settling velocity that would be independent of the exponentially decreasing distribution of more rapidly settling (i.e., coarser) sediment.

The result of the transport calculation in the estuary is plotted with the estimated input from the river based on the rating curve (Fig. 9, note that in this plot, negative indicates down-estuary). Two major seaward flux events are evident, corresponding to the first two river outflow events. Each of these events resulted in a southward transport of approximately 40,000 tons, comparable to the annual average loading from the river. In contrast, the two later discharge events in May had minor impacts on sediment transport, due to the much lower mean concentrations of suspended sediment at the mooring location during those events (Fig. 9, bottom panel). During the low-discharge periods, the net sediment transport was northward (i.e., up-estuary), due to the landward near-bottom flow associated with the estuarine circulation. The cumulative landward transport during low-discharge periods equaled or exceeded the transport during the seaward pulses with river discharge. The calculations show that the net sediment transport is highly variable in time and the quantity of sediment in motion is much larger than the fluvial input. Over the period of observations a large mass of sediment was sloshing back and forth along the estuary, its direction of transport was determined by the strength of the river outflow and the location of the salt intrusion.

Net sediment transport was also calculated for the side embayments at Mendall Marsh and the Orland River, to determine if there is evidence for sediment trapping in side embayments. Based on the moored

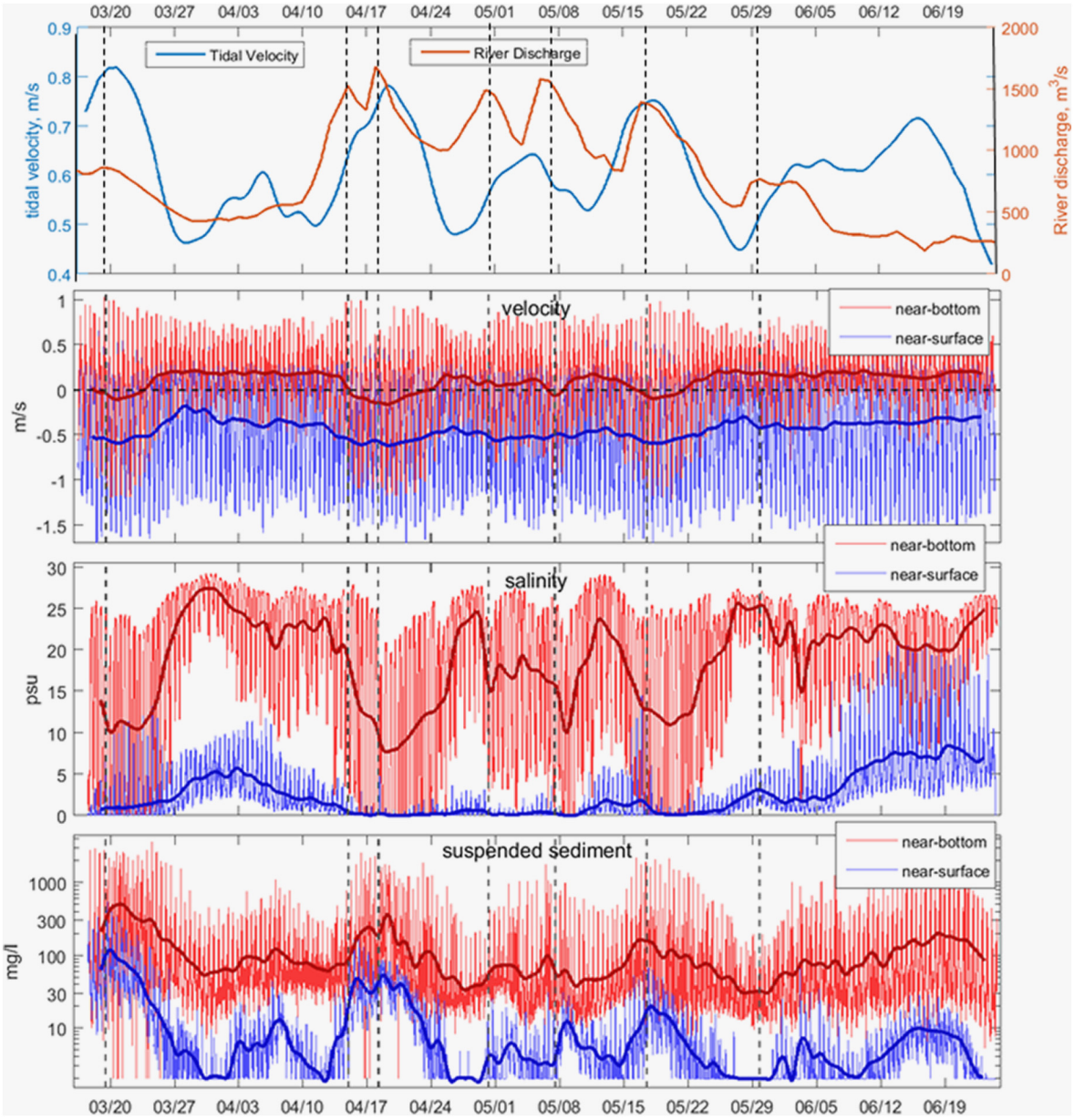

Fig. 7. Time series of moored measurements of salinity, velocity and suspended sediment at the mooring in the Penobscot channel adjacent to Frankfort Flats during the spring of 2011. The upper panel shows tidal velocity amplitude (blue) and river discharge (orange) over the 2011 measurement period. The other panels correspond to near-bottom (red) and near-surface (blue) velocity (2nd panel), salinity (3rd panel) and suspended sediment (bottom panel). The high-frequency fluctuations are due to tidal oscillations. The thick lines are 35-h filtered data that remove the influence of tides. The dashed lines indicate times of peak Penobscot River outflow. (For interpretation of the references to color in this figure legend, the reader is referred to the web version of this article.)

measurements of 2010, the calculated fluxes (Fig. 10) show much less sediment mass in motion than the main stem, but given the small size of these embayments the transport is significant for sediment accumulation. In both Mendall Marsh and the Orland River, the net sediment transport over the measurement period was strongly landward (into the embayments), with outflow only during high discharge in the first half of April (Fig. 3). Seaward river velocities produced net sediment outflow in the side embayments, just like the main stem of the Penobscot. What differs about these side embayments is the strength and persistence of the sediment inflow following the freshet. This sediment inflow is consistent with the hypothesis that the side embayments are sinks of sediment that originated in the Penobscot, as suggested by the steady accretion of contaminated sediment in the Mendall marsh (Santschi et al., 2017).

3.6. Surficial sediment characteristics

Bed sediment samples collected during August 2011 reflect the considerable heterogeneity in surficial sediment characteristics (Fig. 11), with muddy sediment somewhat more prevalent than sand, gravel and rocks. Of the muddy sediment, two distinct types were readily identifiable, one being soft, unconsolidated mud that was light gray to brown, and the other being more firmly consolidated mud that was gray to black and usually smelled of hydrogen sulfide. The organic fraction was higher in the fine sediment, with loss-on-ignition values in the range of 10–20% for the samples that were dominated by fines. Wood chips were also found in some of the samples, most notably near Bucksport where a pulp mill is located. Often the wood chips were associated with unconsolidated mud. Some of the samples included both

Table 1
Classification of grab samples.

Category	Description
1	Unconsolidated mud
2	Consolidated mud
3	Mix of unconsolidated mud and anything else
4	Mixed mud, sand, shells, rocks, wood chips
5	Mussels with rocks and consolidated mud
6	Sand with mud
7	Sand
8	Sand with rocks, shells, wood chips, mussels
9	Gravel with rocks or hard bottom (no sample)
10	Wood chips with unconsolidated mud

unconsolidated mud and other material such as sand, gravel, rocks, and shells (indicated as "mixed" in Fig. 11). A total of 10 categories of sediment were identified, as described in Table 1.

Other studies (e.g., Woodruff et al., 2001) have found based on comparison with the short-lived radionuclide Be-7 that the color and texture of estuarine mud is indicative of its depositional history. Light colored muds, whose color is indicative of oxidation of the iron minerals, are associated with recent deposition (timescales of months). Black and dark gray muds, whose color indicates reduced iron, have been buried long enough for the reduction of iron to have occurred after deposition and isolation from oxygenated water, representing a timescale of many months to years.

Based on the above characterization, the unconsolidated mud, mixed samples and wood chips were all interpreted as part of the mobile sediment pool, which has been resuspended and deposited on timescales of months. This mobile sediment is distributed throughout the estuary, most consistently in low-energy zones such as the east side of Verona Island, but also in frontal trapping zones noted in the shipboard surveys based on the occurrence of salinity fronts and elevated suspended sediment concentrations (Figs. 5–6).

The occurrence of unconsolidated mud in the upper reaches of the estuary in August 2011 was surprising, because in June 2010 all of the samples obtained north of Winterport were found to be coarse sediment, with no mud. The observations suggest a shift in availability of fine sediment in the upper estuary, but because only 3 samples were obtained north of Winterport in 2010 this is not a robust test of change between the sampling periods. The sediment flux calculations are consistent with a seasonal shift in fine sediment into the upper estuary, as during low discharge periods (e.g., summer 2011) the dominant direction of sediment transport is up-estuary (Fig. 9). Moreover, the suspended sediment concentration regression analysis (Fig. 8) suggests

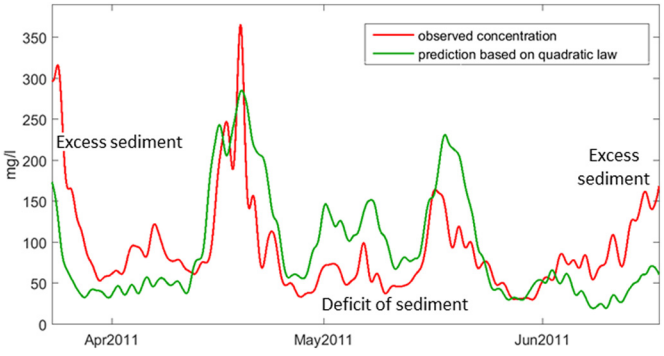

Fig. 8. Comparison of observed near-bottom concentration to a quadratic model based on the near-bottom velocity, showing that the observations show excess suspended sediment relative to the model during the beginning and end of the record, and a deficit of suspended sediment during the middle of the record. These changes in the relationship between tidal velocity and suspended sediment concentration indicate variations in erodibility that may be explained by migration of the mobile pool of sediment.

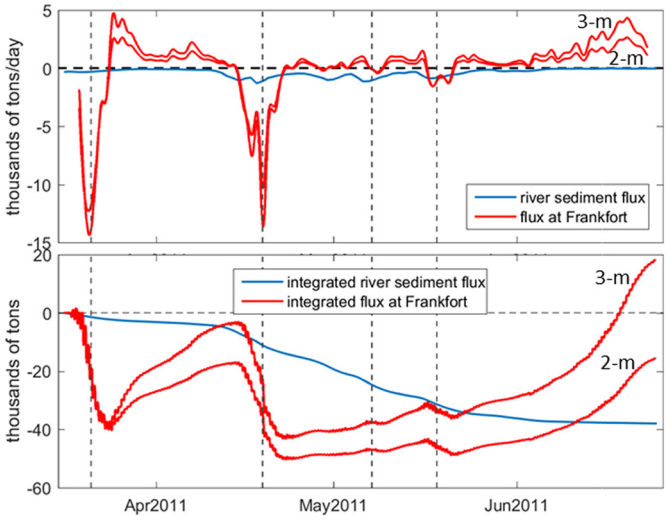

Fig. 9. Estimated sediment flux at the Frankfort Flats mooring in 2011 (red) compared to the estimated flux of the river. Negative indicates out-estuary. Two estimates are shown, one assuming a 2-m vertical e-folding scale of the suspended sediment, and the other with a 3-m scale. The dashed lines show the times of peaks in river outflow. The first two peaks are associated with large out-estuary transport of sediment, but the 3rd and 4th outflow peaks have much weaker suspended sediment transport. This suggests that the mobile pool is transported southward by the initial pulses of discharge, after which there is little sediment in the upper estuary to be transported. (For interpretation of the references to color in this figure legend, the reader is referred to the web version of this article.)

that the fine sediment is depleted from the upper estuary during high discharge periods when the reference concentration for tidal resuspension decreases. Given that the unconsolidated sediment found in the upper estuary is easily eroded, it is likely that this sediment was transported northward from the middle estuary over several months following the freshet.

Additional evidence for seasonal variation in the pool of mobile sediment comes from the burial of the tripod at the Bucksport mooring site during the spring 2011 observations, and its subsequent exhumation in August. Based on the height of the tripod and the fact that it was undetectable by a diver, the mobile sediment apparently extended to at least 1-m depth at that location. Bucksport is the location of intense frontal trapping based on the suspended sediment data (Fig. 5), and the burial of the tripod at this location supports the idea that frontal trapping leads at least locally to substantial, temporary sediment accumulation. The exhumation of the tripod in August is consistent with a northward shift of the mobile sediment pool, as indicated by the suspended sediment flux data (Fig. 10) that indicate a strong northward flux during periods of low river discharge.

3.7. Mercury distribution in grab samples

Mercury concentrations were obtained for all of the bed sediment samples from August 2011. The dry-weight mercury concentration was found to be correlated to the fraction of fine sediment, with a best-fit power-law.

$$Hg \propto (\text{Fine fraction})^{0.6} \quad (2)$$

with $r^2 = 0.65$ for 200 samples. To remove the influence of grain size on the analysis of mercury distributions, the samples were normalized using the relation.

$$Hg_n = Hg/(\text{Fine fraction})^{0.6} \quad (3)$$

where Hg_n is the normalized concentration, approximately representing the concentration of a sample if it were 100% fine

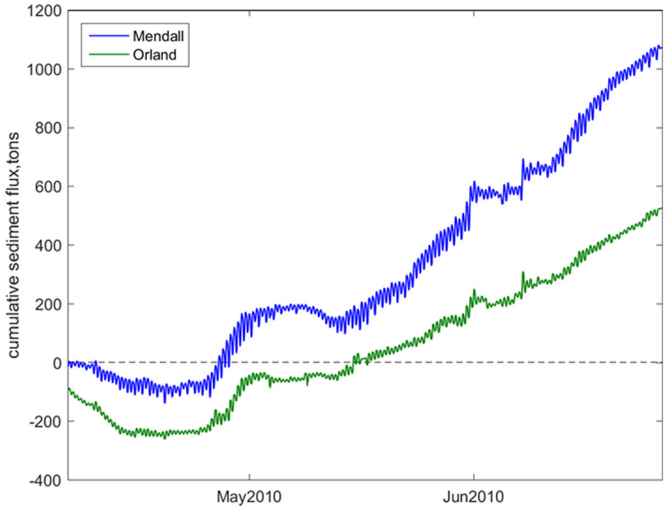

Fig. 10. Estimated integrated sediment transport in Mendall Marsh (blue) and Orland River (green) during the spring of 2010. Early in the observation period, the transport was outward (towards Penobscot River), but over the rest of the observations the transport was into these side-estuaries, indicating trapping of sediment in these lateral embayments. (For interpretation of the references to color in this figure legend, the reader is referred to the web version of this article.)

sediment. The exponent was determined by optimizing the regression between mercury and fine sediment concentration. The normalized concentrations ranged from 200 to 5000 ng/g, with the median around 1000 ng/g. A notable finding was that the variability of Hg concentration was much less in the unconsolidated sediment samples (category 1), with a standard deviation of 299 ng/g (52 samples), compared to all of the other sediment types that had a standard deviation of 1444 ng/g (148 samples) (Fig. 12). The normalized Hg concentration of the unconsolidated sediment was relatively uniform along the estuary, with the exception of the southernmost samples that had lower concentrations (around 600 ng/g compared with 1000 ng/g). Several samples in the channel southeast of Verona Island also showed more variability, both higher and lower, than the other unconsolidated samples. The normalized Hg concentration in other categories of sediment (including all sediment classifications other than the unconsolidated) varied spatially corresponding with the distribution of sediment types. Most of the highest normalized Hg concentrations were found between Winterport and the north end of Verona Island, and the concentrations decreased markedly to the south of Verona Island.

The relatively uniform concentrations of the unconsolidated sediment, as well as the absence of distinct spatial structure through most of the estuary, is consistent with the concept of a mobile pool of sediment that becomes nearly homogenized in Hg concentration due to multiple cycles of remobilization and transport up and down the estuary. Some variability of concentration of the unconsolidated sediment is readily explained by incomplete mixing of the mobile sediment due to spatial and temporal variability in resuspension, as well as intermittent contributions due to introduction of sediment with higher or lower mercury concentrations.

3.8. Sediment and contaminant deposition in Mendall Marsh

Mendall Marsh is one of the most important sites of contamination in the study area, because of the high concentrations of methylated mercury (Gilmour et al., submitted manuscript) and its impact on song-birds that feed on insects in the marsh (Kopec et al., This volume). The sediment cores obtained in the marsh as part of the study indicate uniform rates of accretion of mercury-contaminated sediment of roughly 0.7 cm/y (Santschi et al., This volume). The grab samples containing unconsolidated sediments within Mendall Marsh (Fig. 13) showed Hg concentrations similar to the mean of all of the

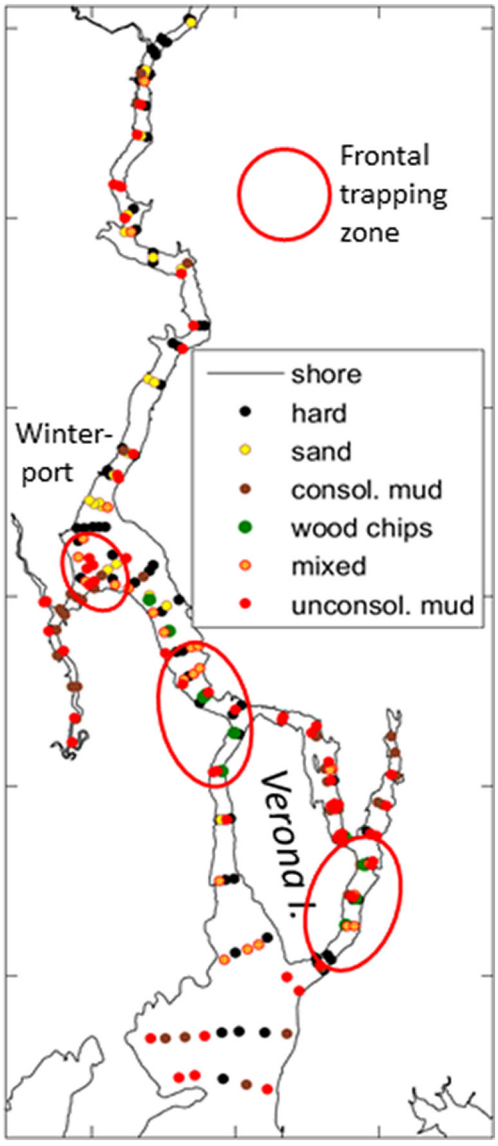

Fig. 11. Distribution of the different categories of sediment from the surface sediment sampling in 2011. The frontal trapping zones are indicated as red circles. (For interpretation of the references to color in this figure legend, the reader is referred to the web version of this article.)

unconsolidated sediments in the greater Penobscot estuary—1084 ± 235 ng/g for Mendall Marsh compared with 897 ± 255 ng/g for all of the unconsolidated sediments (category 1). This suggests that the sediment being transported into Mendall Marsh is part of the mobile pool of relatively homogeneous Hg concentrations. One of the main frontal trapping zones of the Penobscot estuary is found adjacent to the mouth of Mendall Marsh (Figs. 5, 6), which provides a persistent source of mobile sediment to enter the marsh.

Given the likely connection between the sediments of the mobile pool and the sediments accumulating in Mendall Marsh, the depositional record in Mendall Marsh may provide an indication of the historical variation of the concentration of mercury within the mobile pool Santschi et al. (This volume) used the relative distributions of Cs-137 and Hg in cores to determine that Hg concentrations reached a maximum in the early 1970s, with a significant decrease since that time. It is therefore likely that the mercury contamination of the mobile pool followed a similar temporal trajectory, with a peak in the early 1970s and long-term decrease since the industrial discharge was attenuated in the mid-1970s (Bodaly et al., this volume). It is notable that the

Fig. 12. Photographs of different types of sediment in the grab-sampler. The distance across the pictures is approximately 10 cm.

decrease of mercury concentration in Mendall Marsh occurred over decades, even though the input to the Penobscot was abruptly shut off in the 1970s. This long recovery timescale may be explained by the large reservoir of contaminated sediments in the estuary associated with the mobile pool, as explored in the following analysis.

3.9. Timescale of dilution of contaminants in the mobile pool

The expected natural attenuation rate of mercury contamination in the mobile pool depends on size of the mobile pool as well as the rates of input and loss of contaminants and sediment. The size of the mobile pool was estimated from the spatial distribution of sediment grab samples. The mobile pool was defined based on the occurrence of either unconsolidated mud or wood-chips in a sample, excluding the samples in the southern part of the domain with relatively low mercury concentrations. The areal distribution of the unconsolidated mud is reasonably well resolved by the grab sampling, but its depth was not well known. In some cases, the unconsolidated mud extended over the entire 10-cm depth of the grab sample, and in other cases it only constituted several cm at the top. For the purpose of estimating the mass, we assumed that on average, the unconsolidated mud was 5 cm thick. The uncertainty of that estimate is probably a factor of 2—i.e., it is probably not less than 2.5 cm and not more than 10 cm, averaged over the entire estuary. The estuary was divided into 12 segments based on the bathymetric transitions and the area of each segment was calculated from a numerical planimetric calculation (Table 2).

The annual input of sediment to the estuary was determined from the rating curve (Fig. 2) and the long-term discharge estimates at West Enfield, leading to an estimate of 44,000 tons per year. We assume that the new sediment entering the estuary becomes well mixed with the sediment of the mobile pool, and then an equal quantity (on average) is lost from the mobile pool, either by export or burial. This yields a simple estimate of the residence time of sediment.

$$T_{res} = M_{mobile}/F_{river} \tag{3}$$

where T_{res} is the residence time, M_{mobile} is the mass of the mobile pool, and F_{river} is the mass loading of sediment from the river (tons/year). Using the above values, T_{res} amounts to 7.3 ± 3.6 years, where the uncertainty is due mainly to the uncertainty in the thickness of the unconsolidated sediment.

This estimate of sediment residence time may differ somewhat from the dilution timescale of mercury. If the incoming sediment had no mercury, and if there were no additional sources of mercury to the mobile pool, the timescale of mercury dilution would be the same as the sediment residence time. However, the sediment entering from the Penobscot River has some background mercury concentration, and additional mercury enters the mobile pool due to the episodic remobilization of contaminated sediment that had been previously buried. A timescale for mercury dilution was estimated by considering these two sources of mercury to the mobile pool, with the assumption that the mass of sediment in the mobile pool remains constant (i.e., riverine and remobilization inputs equal burial and export). The validity of the steady-state assumption is discussed below. Based on this steady-state balance with both riverine and remobilized sediment input, a timescale of mercury attenuation is determined as follows:

$$T_{Hg} = \frac{M_{mobile} C_{mobile}}{F_{river}(C_{mobile} - C_{river}) + F_{remob}(C_{mobile} - C_{remob})} \tag{4}$$

where T_{Hg} is the dilution timescale for mercury (the time for its concentration to decrease by e^{-1} or to 37% of its original value), F_{remob} is the mass loading of remobilized sediment, and C_{remob} is the average mercury concentration of the remobilized sediment. The average concentration of the sediment entering from the Penobscot River was estimated by Turner et al. (this volume) to be 400 ng/g. The average concentration of the consolidated sediment in the middle estuary (normalized to fine sediment concentration) is 1500 ± 1500 ng/g. This compares with a fine-normalized concentration of the mobile pool of 1024 ± 300 ng/g. Three different values of F_{remob} were selected, representing 5, 10 and 15% of the mass of the mobile pool per year. The corresponding recovery timescales for mercury from Eq. (4) are 12, 18 and 31 years. The

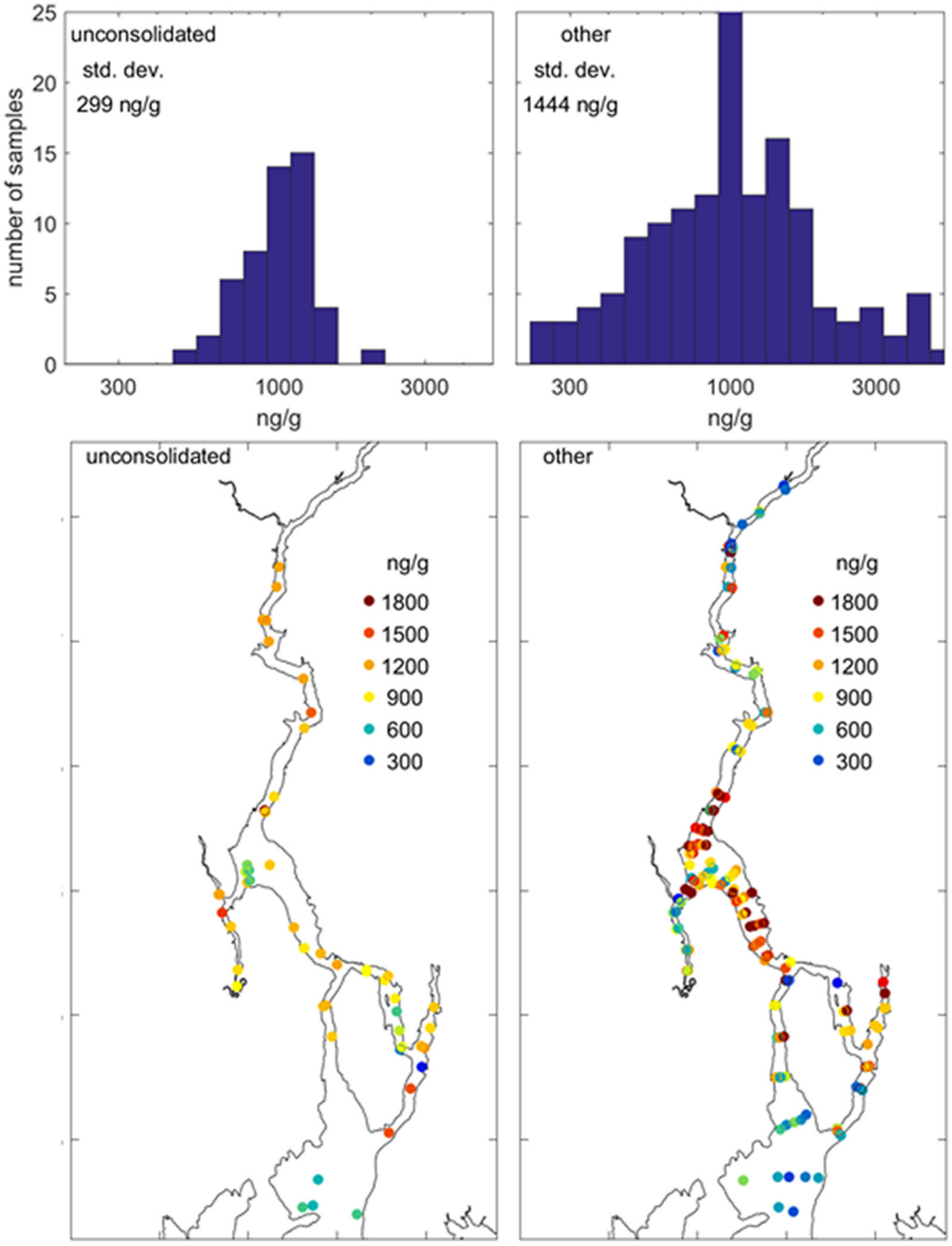

Fig. 13. Comparison of mercury concentrations of unconsolidated sediments (left panels) with consolidated sediment (right panels). Upper panels are histograms, and lower panels show the spatial distributions. The most notable difference between the unconsolidated and consolidated sediments is the much smaller standard deviation of the unconsolidated sediments, suggesting more homogenization.

recovery timescale based on the Mendall Marsh mercury chronology is about 25 years (Santschi et al., This volume), which is consistent with a remobilization fraction between 10 and 15%. Some addition of previously consolidated sediment to the mobile pool is to be expected, because of the temporal and spatial variability of the sediment erosion processes associated with seasonal and interannual variability of the physical forcing. However the distinct difference in the statistical distributions of mercury concentration between the mobile pool and the consolidated sediment suggests that the annual input due to remobilization cannot be large, because the mobile pool has a relatively uniform mercury concentration compared with the more variable concentration of consolidated sediment.

3.10. Mass balance and the steady state assumption

The above calculation is based on the assumption of a steady-state mass of the mobile pool—i.e., the input of sediment from the river and remobilization of bottom sediment equals burial and export. The measurements do not provide adequate precision to assess whether or not the assumption is valid, so it must be based on a consideration of the variability of the forcing, including the supply of sediment from the watershed and the processes affecting remobilization. Interannual variability in the long-term record of river discharge (Fig. 3) is moderate but not extreme, so variations in input are not expected to lead to significant unsteadiness in the long-term sediment balance. Likewise

Table 2
Calculation of mass of mobile pool.

Segment	Area, km^2	Fraction unconsolidated mud[a] or wood-chips	Mass in tons[b]
Upper	5.47	0.28	38,000
Winterport	2.47	0.18	11,400
Mendall	1.38	0.27	9300
Frankfort	5.21	0.31	40,500
Bucksport	4.95	0.46	57,000
Verona west	7.88	0.33	65,700
Verona east	2.99	0.68	50,800
Orland	2.33	0.38	22,400
Verona south	1.99	0.46	22,900
Total	34.67		317,000

[a] Assumes that mixtures of new mud and other material have ½ new mud.
[b] Assumes 5 cm thickness, 500 kg/m^3 bulk density.

remobilization processes are relatively uniform from year to year, as the bottom stress depends mainly on tidal and fluvial processes. The input of sediment from the watershed is relatively well constrained by discharge and suspended sediment data, amounting to a long-term rate of 40,000–50,000 tons/year (cf. Fig. 4), but the other terms in the mass balance are less well constrained. Burial of sediment can be expected to roughly follow sea-level rise in an estuary in a state of morphological equilibrium (Klingbeil and Sommerfield, 2005). Considering a regional sea-level rise of approximately 2 mm/y (NOAA, 2017), an area of 35 km^2 (Table 1), and a bulk density of about 500 kg/m^3, the burial of sediment matching sea-level rise would amount to 35,000 tons/year, close to the watershed input. The amount of export to Penobscot Bay is more poorly constrained. It is not zero, as mercury contamination is evident in the Bay that most likely originated from the estuary (Santschi et al., This volume). Given the low concentration of suspended sediment in the lower estuary compared to in the salt wedge even during high discharge conditions (Fig. 5, also based on low concentrations based on moored measurements of optical backscatter), it is likely that this export is small relative to the input from the river. Based on these albeit rough estimates, the available evidence is in accord with the steady-state approximation for the sediment mass balance.

3.11. Contrast between the mobile pool and the "fluff layer"

Previous studies of the temporary reservoirs of contaminants have focused on the "fluff layer" (Santschi et al., 1990; Adams et al., 1998) or "fluffy layer" (Witt et al., 2001), a layer only a few mm thick of non-cohesive, easily eroded sediment that greatly enhances the exchange of chemicals (including contaminants) between the water column and the surficial sediment (Adams et al., 1998). The distinction can also be considered with respect to timescales—the fluff layer represents the sediment that is remobilized every tidal cycle, whereas the mobile pool is the mass of sediment that is remobilized on seasonal or perhaps even interannual timescales. Although the fluff layer may be considered as part of the mobile pool, the key distinction is that the vertical extent and therefore the mass of the mobile pool may be orders of magnitude greater than the fluff layer, because mobilization of the mobile pool is not simply a result of vertical processes—resuspension and deposition—but also due to persistent, horizontal convergence and divergence of sediment transport due to episodic and seasonal variations in forcing conditions.

3.12. Factors influencing the size of the mobile pool

The vertical scale of the mobile pool in the Penobscot was not known precisely, but the grab sampling suggests an average thickness of unconsolidated sediment of around 5 cm, with local occurrence of much greater thickness, as indicated by the burial of the tripod. Other estuaries show significantly greater thicknesses of remobilized sediment, ranging from 10 to 40 cm in the Hudson (Woodruff et al., 2001) to up to 2 m in the Gironde (Migniot, 1971). The factors determining the size and extent of the mobile pool in the Penobscot were not determined in this study, and the question remains to be addressed in general. Certainly the annual loading of sediment to the estuary is a relevant quantity, as is the magnitude of variation of riverine and tidal forcing and estuarine topography as they influence the variation of the position of sediment trapping zones.

3.13. Contrasting the mobile pool to advection-dominated regimes

A different, but related issue is the timescale of transport of sediment and contaminants through a fluvial, tidal and estuarine dispersal system. A recent observational and modeling study of sediment transport in the Hudson River by Ralston and Geyer (in press) indicates timescales of years to decades for sediment to be transported through the freshwater tidal reaches and saline estuary of the Hudson. This advective timescale should be distinguished from the residence time of the mobile pool, in that the transport processes in the mobile pool are dominantly bi-directional, leading to an effectively diffusive regime when averaged over multiple years. One possible way of distinguishing advective regimes from the mobile pool regime may be the presence or absence of gradients in chemical properties, including contaminant concentrations. The absence of large-scale gradients in mercury concentration within the sediments of the mobile pool in the Penobscot estuary is an indicator of the dominance of horizontal exchange and mixing relative to advection.

4. Conclusions and implications

This key finding of this paper is that a large mass of sediment in the Penobscot estuary is redistributed over seasonal timescales, producing a mobile pool of sediment with relatively uniform contaminant concentrations. The redistribution is due to the variability of the position and strength of sediment trapping zones due to the changes in river flow as well as the spring-neap variability in tidal amplitude. Similar variability in sediment remobilization and the occurrence of a mobile pool of sediments have been found in other estuaries (Wellershaus, 1981; Grabemann and Krause, 2001; Woodruff et al., 2001; Migniot, 1971; Schoellhamer, 2011). The bi-directional transport of sediments in the mobile pool with changing river discharge leads to a homogenization of contaminant concentrations within the mobile pool. The presence of the mobile pool in the Penobscot helps explain the long dilution timescale (roughly 25 years) for mercury contamination in the sediment. This timescale is explained in part by the large mass of the mobile pool compared to the mass of new sediment that enters the estuary from the watershed.

The results of this study have general relevance for understanding and quantifying the fate of contaminants in estuaries, rivers and other water bodies subject to episodic changes in forcing conditions. For example, the PCBs discharged into the Hudson River (Feng et al., 1998) are trapped and remobilized at seasonal and interannual timescales, both in the estuary (Woodruff et al., 2001) and in the tidal river (Ralston and Geyer, in press). The Passaic River estuary provides another example in which contaminants are subject to multiple cycles of trapping and remobilization, resulting in complex spatial distributions and long recovery timescales (Chant et al., 2011; Israelsson et al., 2014). A better understanding of the role of the mobile pool in contaminant fate and transport will lead to improved management and remediation of contaminated estuarine and fluvial environments.

Acknowledgments

The observations and most of the analysis were supported by the Penobscot Mercury Study Panel. Additional support for analysis the preparation of the manuscript were provided by National Science Foundation grant OCE-1634480.

References

Adams, E.E., Stolzenbach, K.D., Lee, J.J., Caroli, J., Funk, D., 1998. Deposition of contaminated sediments in Boston Harbor studied using fluorescent dye and particle tracers. Estuar. Coast. Shelf Sci. 46, 371–382.

Bodaly, N.S. Fisher, C.A. Kelly, A.D. Kopec, J.W.M, Rudd C.G. Whipple 2017 this volume, Mercury Contamination of the Penobscot River Estuary, Maine USA. STOTEN this volume.

Cardona-Marek, T., Schaefer, J., Ellickson, K., Barkay, T., Reinfelder, J.R., 2007. Mercury speciation, reactivity, and bioavalability in a highly contaminated estuary, Berry's Creek, New Jersey Meadowlands. Environ. Sci. Technol. 41, 8268–8274.

Chant, R.J., Fugate, D., Garvey, E., 2011. The shaping of an estuarine superfund site: roles of evolving dynamics and geomorphology. Estuar. Coasts 34, 90–105.

Downing, J., 2006. Twenty-five years with OBS sensors: the good, the bad, and the ugly. Cont. Shelf Res. 26 (17–18):2299–2318. http://dx.doi.org/10.1016/j.csr.2006.07.018.

Feng, H., Cochran, J.K., Lwiza, H., Brownawell, B.J., Hirschberg, D.J., 1998. Distribution of heavy metal and PCB contaminants in the sediments of an urban estuary: the Hudson River. Mar. Environ. Res. 45 (1), 69–88.

Folk, R.L., Ward, W.C., 1957. Brazos River bar: a study in the significance of grain size parameters. J. Sediment. Res. 27, 3–26.

Geyer, W.R., 1993. The importance of suppression of turbulence by stratification on the estuarine turbidity maximum. Estuar. Coasts 16 (1), 113–125.

Geyer, W.R., Farmer, D.M., 1989. Tide-induced variation of the dynamics of a salt wedge estuary. J. Phys. Oceanogr. 19 (8), 1060–1072.

Geyer, W.R., Woodruff, J.D., Traykovski, P., 2001. Sediment transport and trapping in the Hudson River estuary. Estuar. Coasts 24 (5), 670–679.

Gilmour, C.C. et al. 2017, submitted. Methylation of Mercury in the Penobscot River and Estuary, Maine, USA. Submitted to STOTEN.

Grabemann, I., Krause, G., 2001. On different time scales of suspended matter dynamics in the Weser estuary. Estuar. Coasts 24, 688–698.

Grabemann, I., Uncles, R.J., Krause, G., Stephens, J.A., 1997. Behaviour of turbidity maxima in the Tamar (UK) and Weser (FRG) estuaries. Estuar. Coast. Shelf Sci. 45 (2), 235–246.

Hansen, D.V., Rattray, M., 1965. Gravitational circulation in straits and estuaries. J. Mar. Res. 23, 104–122.

Israelsson, P.H., Quadrini, J.D., Connolly, J.P., 2014. Fate and transport of hydrophobic organic chemicals in the lower Passaic River: insights from 2, 3, 7, 8-tetrachlorodibenzo-p-dioxin. Estuar. Coasts 37, 1145–1168.

Klingbeil, A.D., Sommerfield, C.K., 2005. Latest Holocene evolution and human disturbance of a channel segment in the Hudson River Estuary. Mar. Geol. 218 (1), 135–153.

Kopec AD, RA Bodaly and DC Evers 2017. This volume. Mercury in Songbirds Inhabiting a Mercury Contaminated Saltmarsh in the Penobscot River Estuary, Maine USA. STOTEN, this volume.

Kuehl, S.A., DeMaster, D.J., Nittrouer, C.A., 1986. Nature of sediment accumulation on the Amazon continental shelf. Cont. Shelf Res. 6 (1–2), 209–225.

Lerczak, J.A., Geyer, W.R., Ralston, D.K., 2009. The temporal response of the length of a partially stratified estuary to changes in river flow and tidal amplitude. J. Phys. Oceanogr. 39 (4), 915–933.

Maa, J.P.Y., Sanford, L., Halka, J.P., 1998. Sediment resuspension characteristics in Baltimore harbor, Maryland. Mar. Geol. 146 (1), 137–145.

MacCready, P., Geyer, W.R., 2010. Advances in estuarine physics. Annu. Rev. Mar. Sci. 2, 141–162.

Mason, R.P., Lawson, N.M., Lawrence, A.L., Leaner, J.J., Lee, J.G., Sheu, G.R., 1999. Mercury in the Chesapeake Bay. Mar. Chem. 65, 77–96.

Migniot, C., 1971. L'e´volution de la Gironde ou cours des temps. Bull. Inst. Géol. Bassin Aquitaine 11, 211–281.

Nash, D.B., 1994. Effective sediment-transporting discharge from magnitude-frequency analysis. J. Geol. 102 (1), 79–95.

NOAA, 2017. https://tidesandcurrents.noaa.gov/sltrends/sltrends_station.shtml?stnid=8413320.

Partheniades, E., 1965. Erosion and deposition of cohesive soils. J. Hydraul. Div. 91 (1), 105–139.

Postma, H., 1967. Sediment transport and sedimentation in the estuarine environment. In: Lauff (Ed.), Estuaries. Am. Ass. Adv. Sci.

Ralston, D.K. and W.R. Geyer. 2017 Sediment transport timescales and trapping efficiency in a tidal river J. Geophys. Res., in press.

Ralston, D.K., Geyer, W.R., Lerczak, J.A., 2010. Structure, variability, and salt flux in a strongly forced salt wedge estuary. J. Geophys. Res. Oceans 115. http://dx.doi.org/10.1029/2009JC005806.

Santschi, P., Höhener, P., Benoit, G., Buchholtz-ten Brink, M., 1990. Chemical processes at the sediment-water interface. Mar. Chem. 30, 269–315.

Santschi, P.H., Yeager, K.M., Schwehr, K.A., Schindler, K.J., 2017. This volume. Estimates of Recovery of the Penobscot River and Estuarine System from Mercury Contamination in the 1960s. STOTEN, this volume.

Schoellhamer, D.H., 2011. Sudden clearing of estuarine waters upon crossing the threshold from transport to supply regulation of sediment transport as an erodible sediment pool is depleted: San Francisco Bay, 1999. Estuar. Coasts 34, 885–899.

Schubel, J.R., 1968. Turbidity maximum of the northern Chesapeake Bay. Science 161 (3845), 1013–1015.

Traykovski, P., Geyer, R., Sommerfield, C., 2004. Rapid sediment deposition and fine-scale strata formation in the Hudson estuary. J. Geophys. Res. Earth Surf. 109, F02004. http://dx.doi.org/10.1029/2003JF000096.

Turner R.R., A.D. Kopec, M. Charette, P.B. Henderson 2017. this volume. Current and Historical Rates of Input of Mercury to the Penobscot River, Maine, from a Chlor-alkali Plant. STOTEN this volume.

Valentine, K., G.C. Keneke, D.K. Ralston, C.R. Sherwood and W.R. Geyer, 2017 submitted. Response of sediment grain size and bedforms to changing flow conditions in a shallow, energetic estuary. Submitted to Marine Geology.

Wellershaus, S., 1981. Turbidity maximum and mud shoaling in the Weser estuary. Arch. Hydrobiol. 92, 161–198.

Williams, G.P., 1989. Sediment concentration versus water discharge during single hydrologic events in rivers. J. Hydrol. 111, 89–106.

Witt, G., Leipe, T., Emeis, K.-C., 2001. Using fluffy layer material to study the fate of particle-bound organic pollutants in the southern Baltic sea. Environ. Sci. Technol. 35, 1567–1573.

Woodruff, J.D., Geyer, W.R., Sommerfield, C.K., Driscoll, N.W., 2001. Seasonal variation of sediment deposition in the Hudson River estuary. Mar. Geol. 179 (1), 105–119.

Woodruff, J.D., Martini, A.P., Elzidani, E.Z., Naughton, T.J., Kekacs, D.J., MacDonald, D.G., 2013. Off-river waterbodies on tidal rivers: human impact on rates of infilling and the accumulation of pollutants. Geomorphology 184, 38–50.

Yellen, B., Woodruff, J.D., Ralston, D.K., MacDonald, D.G., Jones, D.S., 2017. Salt wedge dynamics lead to sediment trapping within side-embayments in high-energy estuaries. J. Geophys. Res. Oceans http://dx.doi.org/10.1002/2016JC012595.